Published in final edited form as:
Mol Cell. 2010 November 12; 40(3): 465–480. doi:10.1016/j.molcel.2010.10.021.

A stress-responsive system for mitochondrial protein degradation

Jin-Mi Heo[1], **Nurit Livnat-Levanon**[2,9], **Eric B. Taylor**[1,9], **Kevin T. Jones**[3,8,9], **Noah Dephoure**[4], **Julia Ring**[5], **Jianxin Xie**[6], **Jeffrey L. Brodsky**[7], **Frank Madeo**[5], **Steven P. Gygi**[4], **Kaveh Ashrafi**[3], **Michael H. Glickman**[2], and **Jared Rutter**[1,*]

[1]Department of Biochemistry, University of Utah School of Medicine, Salt Lake City, UT, 84112

[2] Department of Biology and The Russell Berrie Nanotechnology Institute, Technion, Israel Institute of Technology, 32000 Haifa, Israel

[3]Department of Physiology and UCSF Diabetes Center, University of California, San Francisco, CA 94158-2517

[4]Department of Cell Biology, Harvard University Medical School, 240 Longwood Avenue, Boston, MA 02115

[5]Institute of Molecular Biosciences, Department of Microbiology, Karl-Franzens-University of Graz, Graz, Austria

[6]Cell Signaling Technology, Inc., Danvers, MA01923

[7]Department of Biological Sciences, University of Pittsburgh, Pittsburgh, PA 15260

Abstract

We show that Ydr049 (renamed VCP/ Cdc48-associated Mitochondrial Stress-responsive—Vms1), a member of an unstudied pan-eukaryotic protein family, translocates from the cytosol to mitochondria upon mitochondrial stress. Cells lacking Vms1 show progressive mitochondrial failure, hypersensitivity to oxidative stress and decreased chronological lifespan. Both yeast and mammalian Vms1 stably interact with Cdc48/ VCP/ p97, a component of the ubiquitin/ proteasome system with a well-defined role in endoplasmic reticulum-associated protein degradation (ERAD), wherein misfolded ER proteins are degraded in the cytosol. We show that oxidative stress triggers mitochondrial localization of Cdc48 and this is dependent on Vms1. When this system is impaired by mutation of Vms1, ubiquitin-dependent mitochondrial protein degradation, mitochondrial respiratory function and cell viability are compromised. We demonstrate that Vms1 is a required component of an evolutionarily conserved system for mitochondrial protein degradation, which is necessary to maintain mitochondrial, cellular and organismal viability.

*To whom correspondence should be addressed: rutter@biochem.utah.edu.
[8]Present address: Department of Molecular, Cell and Developmental Biology, University of California, Los Angeles, CA 90095, USA
[9]These authors contributed equally to this work.

Introduction

Mitochondria are dynamic and complex organelles that are essential for many aspects of cellular function including metabolism and cell death. Consistent with these critical roles, mitochondrial dysfunction is associated with most aging-related human diseases, including neurodegenerative disorders, type 2 diabetes and cancer (Wallace, 2005). The best current inventory of mammalian mitochondrial resident proteins consists of 1098 proteins (Pagliarini et al., 2008). Surprisingly, nearly 300 of these proteins have completely undefined functions, including many that are highly conserved throughout eukarya, indicating that they perform a fundamental and important function (Meisinger et al., 2008; Pagliarini et al., 2008). The genes that encode the mitochondrial proteome are heavily represented amongst known human disease genes, with about 20% of predicted human mitochondrial proteins implicated in one or more hereditary diseases (Andreoli et al., 2004; Elstner et al., 2008). Presumably, the quarter of the mitochondrial proteome that is uncharacterized contains other proteins with links to human disease that await discovery. Making these connections would be greatly facilitated by an understanding of the biochemical and physiological function of these proteins.

Therefore, we initiated studies to determine the genetic and biochemical functions of a subset of these conserved but uncharacterized mitochondrial proteins (Hao and Rutter, 2009). As a result of this project, we previously identified the unstudied Yol071 yeast protein, which we named Sdh5, as a critical assembly factor for the succinate dehydrogenase complex/ complex II (Hao et al., 2009). By virtue of this observation, we identified the human *SDH5* ortholog as the causative gene in a familial form of the paraganglioma neuroendocrine tumor syndrome (Hao et al., 2009). We describe herein another unstudied conserved mitochondrial protein, Ydr049, which we now designate VCP/ Cdc48-associated Mitochondrial Stress-responsive 1 (Vms1). *VMS1* is highly evolutionarily conserved, with one ortholog existing in most eukaryotic species. Initially using yeast, we show that Vms1 protects mitochondrial respiratory function and combats cell death in response to various stress stimuli. Both yeast and human Vms1 co-purify with Cdc48/ VCP/ p97 and we show that Vms1 stably associates with both Cdc48 and its cofactor Npl4, which have well defined roles in the degradation of endoplasmic reticulum (ER) proteins by the proteasome. We find that Cdc48 recruitment to mitochondria is Vms1-dependent and this system is required for normal mitochondrial protein degradation under stress conditions.

Clear links between mitochondria, which are membrane confined organelles, and the cytosolic ubiquitin/ proteasome system have recently been described (Livnat-Levanon and Glickman, 2010). Fzo1, a mitochondrial outer membrane protein, was shown to be ubiquitinated by the Mdm30 cytosolic E3 ubiquitin ligase and degraded by the proteasome (Cohen et al., 2008; Fritz et al., 2003). Mitochondria in cells lacking *MDM30* aggregate in clumps and respire inadequately, leading to shortened lifespan in response to stress. This is likely a manifestation of a broader system for degradation of mitochondria-associated proteins. The flux of imported proteins and the proximity to oxidative phosphorylation result in significant protein damage and misfolding at mitochondria, necessitating a responsive quality control system. The mitochondria contains a intrinsic system of proteases dedicated to quality control (Tatsuta, 2009), but the cytosolic ubiquitin/ proteasome system appears to also play a role. Based on the data presented herein, we propose that Vms1 plays a conserved role in recruiting the ubiquitin/ proteasome system for stress-responsive mitochondrial protein degradation.

Results

Vms1 necessity and mitochondrial translocation under conditions of mitochondrial stress

The Vms1 protein was detected by mass spectrometry in highly purified mitochondria (Sickmann et al., 2003). Surprisingly, however, a functional Vms1-GFP fusion localized primarily to the cytosol in synthetic glucose-containing medium (Figure 1A top) as well as rich and synthetic media containing glycerol and raffinose (data not shown). In a small fraction of cells grown in synthetic glucose medium, Vms1-GFP partially colocalized with the mitochondrial marker mito-RFP (Figure 1A top, marked with arrow). Hypothesizing that this small population might be cells that have lost mitochondrial DNA (*rho*^{o}), we directly tested a *rho*^{o} strain and found that Vms1 was partially mitochondrial in all cells (Figure 1A). Loss of mitochondrial DNA has a number of effects on mitochondrial physiology, including decreased mitochondrial membrane potential (Petit et al., 1996). The combination of Antimycin A and oligomycin, which blocks the establishment of the mitochondrial membrane potential (Priault et al., 2005), caused near complete localization of Vms1 to mitochondria (Figure S1A). Treatment with the uncouplers CCCP or FCCP, which directly dissipate the membrane potential, also caused mitochondrial localization of Vms1 (Figure S1A).

We also found that oxidative stress, which indirectly impairs mitochondrial function, elicited by hydrogen peroxide or deletion of the mitochond rial superoxide dismutase, Sod2 caused mitochondrial translocation of Vms1 (Figure 1A and data not shown). Hydrogen peroxide also caused Vms1-GFP localization to punctae that do not have mito-RFP, which may be damaged mitochondria that fail to import mito-RFP. Treatment with the TOR protein kinase inhibitor rapamycin, which increases mitochondrial oxidative damage (Kissova et al., 2006), also caused robust mitochondrial translocation of Vms1-GFP (Figure 1A). We hypothesize that perturbation of mitochondrial function is the proximal signal that causes Vms1 translocation, with rapamycin and oxidative stress acting indirectly through mitochondrial oxidative damage.

To address the functional significance of Vms1 mitochondrial localization, we analyzed the growth of the *vms1*Δ mutant under conditions that cause Vms1 mitochondrial translocation. While the *vms1*Δ mutant was indistinguishable from wild-type in normal conditions, it exhibited severe hypersensitivity to hydrogen peroxide, an effect exacerbated when combined with loss of the mitochondrial Sod2 (Figure 1B). In fact, the *sod2*Δ *vms1*Δ double mutant exhibited a modest growth defect even on normal medium (Figure 1B top). Similarly, the *vms1*Δ mutant failed to grow in the presence of rapamycin, which was completely rescued by plasmid-borne *VMS1* and partially rescued by expression of the human *VMS1* gene (Figure 1C). This failure to grow is a result of cell death caused by rapamycin treatment (Figure S1B). A high-copy suppressor screen yielded three genes that, when provided in high copy, rescue the *vms1*Δ mutant rapamycin hypersensitivity: *XBP1, GRX3, ZWF1* (Figure S1C,D). Each of the three has a role in response to stress, particularly oxidative stress. Xbp1 is a stress-induced transcription factor. Grx3 is a glutaredoxin and is a component of a major antioxidant system. Loss of Grx3 leads to increased protein oxidation and hypersensitivity to oxidizing agents (Rodriguez-Manzaneque et al., 1999). *ZWF1*-encoded glucose-6-phosphate dehydrogenase produces NADPH, which is essential for the reduction of oxidized glutathione. The *zwf1*Δ mutant is hypersensitive to oxidative stress agents, particularly hydrogen peroxide (Nogae and Johnston, 1990; Outten and Culotta, 2003). These data suggest that Vms1 is required for normal tolerance to oxidative stress and this is manifest by hypersensitivity to both hydrogen peroxide and rapamycin.

Deletion of *VMS1* causes loss of mitochondrial function and viability

During the course of these experiments, we observed that cultures maintained past log phase exhibited mitochondrial Vms1 in the absence of other stressors. For example, maintenance in culture past log phase (e.g. 1.5 d) caused mitochondrial localization of Vms1-GFP (Figure 2A). We confirmed the mitochondrial localization of Vms1-HA by biochemical fractionation after mild cross-linking. Vms1 was detectable in both the cytosolic and crude mitochondrial fractions and a portion of Vms1-HA co-migrated exactly with the mitochondrial marker Tom20 in a sucrose gradient (Figure 2B).

As the *vms1*Δ mutant grows poorly under the same conditions that cause mitochondrial translocation of Vms1, we hypothesized that the primary defect of Vms1 loss involves mitochondrial failure. We tested mitochondrial respiration and the wild-type and *vms1*Δ strains consumed oxygen equivalently in log phase. After 1.5 days of culture, however, the *vms1*Δ mutant had a significant impairment in oxygen consumption (Figure 2C). Due to an exposed iron-sulfur cluster, the activity of aconitase is exquisitely sensitive to mitochondrial oxidative stress. As in the respiration assay, there was no difference in aconitase activity in log phase, but the activity of the *vms1*Δ mutant was significantly reduced relative to wild-type at day 1.5 without a reduction in protein level (Figure 2D and data not shown). We hypothesize that the progressive mitochondrial stress in stationary phase culture necessitates Vms1 for the maintenance of respiration and aconitase activity.

For cells in stationary phase, mitochondrial respiration is required for ATP synthesis and cell survival (Werner-Washburne et al., 1993). Therefore, we sought to determine whether the time-dependent loss of mitochondrial function in the *vms1*Δ mutant might be manifest as a time-dependent defect in colony formation on glycerol medium, wherein ATP generation and growth requires mitochondrial respiration. At day 1.5 of culture, glycerol growth of the *vms1*Δ strain remained similar to the wild-type level (Figure 2E). This suggests that the mitochondrial impairment observed at day 1.5, as manifest by decreased oxygen consumption and aconitase activity, is reversible at this point. In contrast, the *vms1*Δ mutant was greatly impaired in glycerol colony formation at day 3.5 (Figure 2E). By day 5.5, colony formation on glycerol was nearly absent (Figure 2E). After 8.5 days of culture, the *vms1*Δ mutant also showed greatly reduced ability to form colonies on glucose medium (Figure 2E). This is likely due to cell death as we obtained similar results using exclusion of trypan blue as a measure of viability (data not shown). Two independent *vms1*Δ isolates in a different strain background (BY4741) exhibited an even more rapid loss of viability than was observed in the W303 background (Figure 2F). Oxidative stress has been proposed to be the key mediator in causing cell death in static culture (Fabrizio et al., 2001) and the *vms1Δ* mutant showed a significant increase in the oxidation of DHE to ethidium (Figure 2G and Figure S4).

In addition to measuring mitochondrial function and glycerol growth in static culture, we also examined the effect of oxidative stress. As with growth to day 1.5, combination with the *sod2*Δ mutant caused a significant loss of oxygen consumption and aconitase activity in the *vms1*Δ mutant (Figure S5). Similarly, while the *vms1*Δ mutant exhibited normal glycerol growth in the absence of additional stressors, combination with a deletion of *SOD2* caused a complete loss of growth on glycerol medium (Figure 2H). Combined, these data show that the *vms1*Δ mutant has severely compromised mitochondrial activity under the conditions that cause Vms1 mitochondrial translocation.

VMS1 localization and function in *C. elegans*

To determine whether *VMS1* orthologs from other eukaryotes function similarly, we examined *vms-1* in *C. elegans*, which contains a single *VMS1* ortholog encoded by

K06H7.3. Either of two non-overlapping RNAi constructs targeting *vms-1* caused a marked reduction in viability in response to hydrogen peroxide (Figure 3A). The surviving *vms-1*-depleted individuals were dramatically more lethargic than controls. This was confirmed in a mutant line carrying a deletion predicted to remove the majority of the VMS-1 protein (data not shown). Under standard growth conditions, *vms-1* mutants and RNAi-treated animals had normal morphology and wild-type growth and development.

Activation of numerous stress-response genes, including the mitochondrial superoxide dismutase genes *sod-2* and *sod-3,* is dependent on the function of the insulin-regulated FOXO transcription factor DAF-16 (Murphy et al., 2003; Oh et al., 2006). As expected, *daf-16* mutant animals were also hypersensitive to hydrogen peroxide treatment (Figure 3A). Treatment of *daf-16* mutants with *vms-1* RNAi caused further hypersensitivity of similar relative magnitude to that observed in wild-type *vms-1* RNAi treated animals (Figure 3A). Knockdown of *vms-1* also caused a significant decrease in lifespan of wild-type animals and a further decrease in the already-shortened lifespan of *daf-16* mutants (Figure 3B). These findings suggest that *vms-1* functions in parallel with insulin signaling to regulate stress resistance and lifespan.

To determine the tissue and subcellular expression patterns of *C. elegans* VMS-1, we generated transgenic lines in which full-length VMS-1 fused to a GFP reporter was expressed from the native *vms-1* promoter. This reporter was expressed broadly during embryonic development. In larval stages and in adults, expression was noted in intestinal cells, specific neurons in the head and the tail, and in the ventral nerve cord (Figure 3C and Figure S3). In untreated animals, VMS-1::GFP localized to the cytoplasm in intestinal cells and neurons. In head amphid neurons, VMS-1::GFP was uniformly detected in the dendritic processes, where it was specifically excluded from mitochondria, as determined by lack of co-localization with DIC-1::mCherry (Kass et al., 2001) (Figure 3C). Exposure of animals to hydrogen peroxide, however, caused colocalization of VMS-1::GFP with DIC-1::mCherry (Figure 3C), an identical pattern to that seen for other mitochondrial proteins (Hu and Barr, 2005). Together, these findings indicate that, as in yeast, *C. elegans vms-1* function is dispensable for viability and growth but is required for protection against oxidative stress and for wild-type lifespan.

Vms1 constitutively interacts with Cdc48 and Npl4

While the Vms1 protein expressed in *E. coli* migrated as a monomer in gel filtration chromatography, endogenous Vms1 from crude yeast lysates migrated in a large >500 kDa complex (data not shown). To identify subunits of the putative Vms1 complex, we purified a functional Vms1-TAP fusion and identified associated proteins by mass spectrometry. Cdc48, a hexameric AAA-ATPase with a well-studied role in protein degradation (Jentsch and Rumpf, 2007), copurified almost stoichiometrically with Vms1-TAP (Figure 4A)

The Vms1-Cdc48 interaction was confirmed by co-immunoprecipitation of epitope-tagged versions of Vms1 and Cdc48 expressed under their endogenous promoters. Immunoprecipitation of Vms1-HA pulled down Cdc48-myc (Figure 4B). This interaction was also observed following 2 h treatment with rapamycin (Figure S4A), a condition that causes Vms1 mitochondrial translocation. The S565G mutant of Cdc48 was previously reported to cause increased sensitivity to oxidative stress, reduced respiratory activity, and increased cell death (Braun et al., 2006; Madeo et al., 1997). This mutant was expressed at wild-type levels, but interacted much more weakly with Vms1 than did wild-type Cdc48 (Figure 4B). Thus, Vms1 exists in a stable complex with Cdc48 and this interaction is disrupted by a Cdc48 mutation associated with increased oxidative stress sensitivity and cell death. Cell death in Cdc48-S565G mutant strains has been previously shown by increased annexin V and propidium iodide (PI) staining (Madeo et al., 1997). Like Cdc48-S565G

mutant strains, the *vms1*Δ mutant strain had a significantly increased fraction of Annexin V and PI positive cells (Figure S4B,C).

Cdc48 is a component of the ubiquitin/ proteasome system and promotes protein degradation in a variety of cellular contexts, including membrane fusion, cell cycle regulation, transcription factor activation, and ER-associated protein degradation (ERAD) (Bays and Hampton, 2002; Ye, 2006). To carry out these diverse functions, Cdc48 interacts with different cofactor proteins that target Cdc48 activity to distinct cellular sites and also mediate ubiquitin and proteasome binding (Jentsch and Rumpf, 2007). We found that Vms1 also associated with the Cdc48 cofactor Npl4 (Figure 4C) and this interaction was maintained upon rapamycin treatment (Figure S4A). In the same experiment, however, we could not detect an interaction between Vms1 and Ufd1, another Cdc48 cofactor that has been implicated, along with Npl4, in the activity of Cdc48 in ERAD (Figure 4C). To confirm the lack of interaction with Vms1, we tested the ability of Ufd1 to interact with Vms1 and Npl4 in parallel in the same experiment. While Ufd1 exhibited a strong interaction with Npl4 as expected, it failed to interact with Vms1 (Figure 4D). We, therefore, speculate that Vms1 and Ufd1 are mutually exclusive components of the Cdc48-Npl4 complex. This idea is corroborated by high-throughput protein-protein interaction analyses that show both Vms1 and Ufd1 as interacting with Cdc48 and Npl4, but no interaction between Vms1 and Ufd1 (Jensen et al., 2009).

The Vms1 C-terminal region (Figure S4D) was necessary and sufficient for Cdc48 interaction (Figure 4E). For an unknown reason, deletion of the N-terminus actually resulted in increased interaction with Cdc48 relative to wild-type Vms1. The Vms1 interaction with Npl4 exhibited the exact same pattern of domain dependence (Figure 4F). We iden tified a sequence at the extreme C-terminus of Vms1 that showed similarity with the VCP (mammalian Cdc48 ortholog) interaction motif, or VIM, found in the human E3 ubiquitin ligase GP78 and SVIP proteins (Yeung et al., 2008). The putative VIM sequence in yeast Vms1 is highly conserved in Vms1 orthologs (Figure 5A). A mutant lacking this motif (as indicated in Figure 5A) exhibited a wild-type pattern of localization—cytosolic in normal conditions, with mitochondrial translocation in rapamycin and hydrogen peroxide (Figure S5). This mutant, however, completely failed to interact with either Cdc48 or Npl4 (Figure 5B,C), suggesting that Vms1 interacts directly with Cdc48 through a C-terminal VIM sequence and the interaction with Npl4 is mediated by Cdc48.

Specific loss of Cdc48 and Npl4 binding in this mutant enabled us to test whether the genetic function of Vms1 requires interaction with Cdc48 and Npl4. We assayed the ability of wild-type and VIM mutant *VMS1*, expressed from the native promoter, to rescue the rapamycin hypersensitivity of the *vms1*Δ mutant strain. As shown in Figure 5D, wild-type Vms1 rescued fully, but the VIM mutant Vms1 had no effect on growth despite being expressed at levels equivalent to wild-type Vms1 (see Figure 5C). These data suggest that the function of Vms1 required for rapamycin resistance, which we hypothesize relates to protection of mitochondrial function from oxidative damage (see Figure 2), is completely dependent upon interaction with Cdc48.

To identify the protein interactions of mammalian Vms1, we conducted a tandem-affinity purification of a Flag/ HA-tagged mouse Vms1 expressed in mouse C2C12 cells. The final elution had essentially only two bands (Figure 5E), Vms1-Flag/ HA and VCP, the mammalian ortholog of Cdc48. This interaction was confirmed by co-immunoprecipitation experiments. While wild-type Vms1 precipitated endogenous VCP (Figure 5F, lane 6), this interaction was completely lost in a mutant wherein three highly conserved VIM residues (as indicated in Figure 5A) had been mutated to alanine (Figure 5F, lane 9). This experiment was performed quantitatively to enable determination of the amount of VCP that associates

with Vms1. While greater than 90% of the tagged Vms1 was precipitated, we observed essentially no depletion of the total VCP (Figure 5F, compare lanes 4-6), suggesting that the Vms1-associated VCP accounts for less than 5% of the total cellular VCP. The Yeast Vms1 also appears to interact with a similarly small fraction of the total cellular Cdc48 (data not shown). This is consistent with the observation that Cdc48 has a much higher abundance than Vms1 in normal yeast cells (Ghaemmaghami et al., 2003).

Vms1-dependent mitochondrial translocation of Cdc48

Based on the stable and constitutive interaction between Vms1 and both Cdc48 and Npl4, we hypothesized that Vms1 might mediate the recruitment of a subset of Cdc48 and Npl4 to mitochondria. Under normal conditions, Cdc48-GFP localized throughout the cytoplasm, nucleus, and ER (Figure 6A). Upon hydrogen peroxide treatment, however, a fraction of Cdc48-GFP translocated to mitochondria in wild-type cells (Figure 6A). The stress-induced mitochondrial translocation of Cdc48 was nearly absent in a *vms1*Δ mutant strain, but was restored by a plasmid-borne copy of *VMS1* (Figure 6A). Cdc48-GFP also exhibited localization to non-mitochondrial punctae upon hydrogen peroxide treatment that was independent of Vms1. The ratio of Cdc48-GFP that co-localized with mito-RFP versus total cellular Cdc48-GFP was blindly quantitated in these three strains in the presence and absence of hydrogen peroxide. This quantitative analysis showed that loss of *VMS1* largely abrogated the peroxide-induced mitochondrial localization of Cdc48-GFP (Figure 6B). There appears to be, however, a small fraction of Cdc48 that shows stress-responsive mitochondrial colocalization that is independent of Vms1. Our imaging and quantification are currently unable to distinguish whether this is due to an alternative mitochondrial-targeting system or to Cdc48 localization to sites nearby mitochondria. A fraction of Npl4 also exhibits stress-responsive translocation to mitochondria that is dependent on Vms1 (Figure S6).

If Vms1 recruits Cdc48 and Npl4 to increase their local concentration at mitochondria in response to stress, overexpression of Npl4 and/ or Cdc48 might partially complement the *vms1*Δ mutant phenotype by non-specifically increasing their local concentration at mitochondria. As expected, both Cdc48 and Npl4 overexpression suppressed the rapamycin hypersensitivity of the *vms1*Δ mutant strain (Figure 6C). Consistent with the observation that Ufd1 does not associate with Vms1, overexpression of Ufd1 had no effect on the *vms1*Δ mutant phenotype (Figure 6C). Together, these data support a role for Vms1 in recruiting Cdc48 and Npl4 to mitochondria in response to stress, and this activity is a primary function of Vms1.

VMS1 is required for mitochondrial protein degradation

As part of the ERAD machinery, Cdc48 and Npl4 promote the retrotranslocation of lumenal ER or ER membrane proteins to the cytosol where they are degraded by the proteasome in a ubiquitin-dependent manner (Raasi and Wolf, 2007; Vembar and Brodsky, 2008). Under the hypothesis that the Vms1-Cdc48-Npl4 complex functions similarly at mitochondria, we measured the steady state levels of Fzo1. Fzo1 is a mitochondrial outer membrane protein that is the best-characterized mitochondrial target of ubiquitin/ proteasome system-dependent degradation in yeast (Cohen et al., 2008; Escobar-Henriques et al., 2006). While the levels of Fzo1 are identical in wild-type and the *vms1*Δ mutant in log phase (data not shown), the *vms1*Δ mutant exhibited elevated Fzo1 levels at day 2.5 of culture (Figure 7A). The levels of Fzo1 were similar to that found in a mutant lacking Mdm30, the principal ubiquitin E3 ligase involved in Fzo1 degradation (Cohen et al., 2008). The *mdm30*Δ *vms1*Δ double mutant showed an additive effect (Figure 7A).

If the Vms1-Cdc48-Npl4 complex is required for normal Fzo1 degradation, mutants of Cdc48 and Npl4 should also show elevated Fzo1 steady-state levels. The S565G mutant of Cdc48, which exhibits impaired Vms1 binding, had elevated Fzo1 levels similar to the *vms1*Δ mutant (Figure 7B). The Fzo1 levels of the *vms1*Δ *cdc48*-S565G double mutant are similar to the two single mutants, consistent with the proteins acting within the same pathway to promote Fzo1 degradation. Fzo1 also accumulated in the temperature sensitive *npl4-1* mutant at the permissive temperature (Figure S7A), where there is no growth defect on glucose-containing medium (see Figure S7B). Consistent with a role for Npl4 in supporting mitochondrial function, the *npl4-1* mutant grew poorly on glycerol medium, but not glucose medium (Figure S7B).

To directly address the stability of Fzo1, we examined the degradation kinetics of an Fzo1-HA fusion protein following cycloheximide addition to prevent new protein synthesis. Degradation of Fzo1-HA was reproducibly delayed in the *vms1*Δ mutant relative to wild-type cells (Figure 7C—quantitation in Figure S7C). Under identical experimental conditions, the ERAD substrate CPY* was degraded with similar kinetics in the wild-type and *vms1*Δ mutant strains (Figure 7D). In fact, the degradation of CPY* in the *vms1*Δ mutant was slightly enhanced relative to wild-type (Figure 7D), while CPY* was stabilized in a *ufd1-1* mutant (Figure 7E). This is consistent with the idea that Vms1 and Ufd1 compete for interaction with Cdc48 and Npl4. The absence of Vms1 would enable a higher fraction of Cdc48 and Npl4 to associate with Ufd1 and be employed in ERAD.

Based on the nature of the *vms1*Δ mutant phenotype and its association with Cdc48, we reasoned that Vms1 must function more broadly than just mediating Fzo1 degradation. We therefore compared the status of ubiquitinated proteins from wild-type and *vms1*Δ strains at day 1.5 of culture. Cytosolic ubiquitin-protein conjugates were similar in the wild-type and *vms1*Δ mutant strains (Figure 7F). A crude mitochondrial fraction, which is highly contaminated with ER as indicated by the presence of the Cu e1 protein, has a complicated pattern of ubiquitination, with some ubiquitin-protein conjugates being elevated in the *vms1*Δ mutant and others being lower (Figure 7F). When that crude mixture was separated by sucrose-gradient purification to generate more purified mitochondria, however, the *vms1*Δ mutant showed an increased abundance of a subset of ubiquitin-protein conjugates relative to wild-type (Figure 7F, a replicate is shown in Figure S7D). This suggests that the *vms1*Δ mutant might have decreased ubiquitin-protein conjugates in other membrane fractions, particularly the endoplasmic reticulum. The increased abundance of mitochondrial ubiquitin-protein conjugates in the *vms1*Δ mutant is not uniform. Some conjugates are of equal abundance and others are decreased in the *vms1*Δ mutant, consistent with the fact that Cdc48 is important for polyubiquitination in some contexts (Richly et al., 2005).

We hypothesized that Vms1 recruits Cdc48 and Npl4 to mitochondria to engage the ubiquitin-proteasome system in mitochondrial protein degradation. One alternative explanation for the slower protein degradation and increased abundance of ubiquitin-protein conjugates in *vms1*Δ mutant mitochondria is impaired autophagic degradation of mitochondria or mitophagy. fusion protein. In log phase, a mitochondrially-targeted DHFR-GFP reporter is intact and localized to mitochondria (Okamoto et al., 2009) (Figure 7G). Upon induction of mitophagy, however, mitochondria are trafficked to the vacuole and the protein is partially degraded, leaving a protease-resistant GFP fragment. At day 2.5 of culture, both the wild-type and *vms1*Δ mutant showed the processed GFP fragment with the *vms1*Δ mutant actually having higher levels, indicative of increased mitophagy. To address mitophagy in a complementary manner, we determined the levels of a variety of mitochondrial resident proteins. When normalized to the cytosolic protein Pgk1, the *vms1*Δ mutant showed elevated Fzo1 as observed previously (Figure 7H). On the other hand, the mutant showed decreased levels of the mitochondrial proteins Cox1, Cox2, Porin and Rip1

(Figure 7H). The increase in autophagic protein degradation in the *vms1*Δ mutant means that the delayed Fzo1 degradation in the *vms1*Δ mutant is an underrepresentation of the actual impairment in proteasomal degradation of this protein. Mitochondria from the *vms1*Δ mutant show loss of respiratory function and increased oxidative stress and protein ubiquitination, all of which would be predicted to induce mitophagy. We, therefore, hypothesize that the *vms1*Δ mutant has impaired ubiquitin-dependent protein degradation and one of the indirect effects of that is increased mitophagy.

If the *vms1*Δ mutant has impaired proteasomal degradation of mitochondrial proteins, it might be more reliant on internal mitochondrial proteases, like Oma1 and Yme1, for protein quality control. The Oma1 protease, which appears to have little function in unstressed cells, plays a role in mitochondrial integral inner-membrane protein quality control in yeast (Bestwick et al., 2010) and is activated upon mitochondrial dysfunction in mammalian cells (Ehses et al., 2009; Head et al., 2009). Yme1 is the principal subunit of the inter-membrane space i-AAA protease and is responsible for protein degradation in that compartment (Koppen and Langer, 2007). While the *vms1*Δ single mutant showed a slight growth defect on glycerol and the *oma1*Δ mutant had no glycerol growth defect, the *oma1*Δ *vms1*Δ double mutant exhibited a near complete loss of growth on glycerol (Figure 7I). Under these conditions, there was only very slight impairment of growth on glucose, indicating that the phentoype is specific for respirative growth (Figure 7I). A similar synthetic phenotype was observed between the *vms1*Δ mutation and loss of the Yme1 protease (Figure 7J). Together, these data show that Vms1 is required for normal ubiquitin-proteasomal degradation of mitochondrial proteins. In its absence, the cell becomes more reliant on alternative protein degradation strategies, including mitophagy and intrinsic mitochondrial proteases.

Discussion

Herein, we show that Vms1 is part of an evolutionarily conserved mitochondrial stress-responsive system that promotes mitochondrial protein degradation and function. Vms1 is cytosolic in wild-type *S. cerevisiae* cells maintained in normal laboratory conditions. Vms1 translocates to mitochondria, however, in response to a variety of stress stimuli that all impact mitochondrial function. By analogy to the ERAD system that responds to unfolded proteins in the ER, accumulation of damaged, ubiquitinated or partially translocated proteins at mitochondria might signal for recruitment of the Vms1-Cdc48-Npl4 complex. Such a recruitment stimulus would be logical in light of the function of this complex in protein degradation as shown herein.

We provide several lines of evidence that the primary function of Vms1 is the mitochondrial recruitment of a complex containing Cdc48 and Npl4, thereby promoting ubiquitin-dependent protein degradation. First, mitochondrial perturbations cause mitochondrial translocation of Vms1 as demonstrated both by imaging of Vms1-GFP and by detection in gradient-purified mitochondria. Each of the experimental conditions under which the *vms1*Δ mutant exhibits impaired viability or growth, including rapamycin treatment, oxidative stress and static culture, cause mitochondrial translocation of Vms1. This suggests that the function of Vms1, with respect to these phenotypes, is performed at mitochondria.

Second, Vms1 is required for normal mitochondrial recruitment of Cdc48 and Npl4 in response to mitochondrial stress. Only a fraction of Cdc48 and Npl4 are recruited to mitochondria, presumably the same minor population that is Vms1-associated. If, as we propose, the phenotype of the *vms1*Δ mutant is due to a deficiency of Cdc48/ Npl4 in the vicinity of mitochondria, increasing the cellular concentration of these two proteins might rescue that growth defect. Indeed, overexpression of either Npl4 or Cdc48 partially rescued the *vms1*Δ growth defect.

Third, the primary function of Vms1 depends upon interaction with Cdc48. This observation was enabled by the discovery that Vms1 possesses an evolutionarily conserved VCP Interaction Motif (VIM). We showed that deletion of the yeast Vms1 VIM abrogated th e interaction with Cdc48. This same mutation completely destroyed the ability of Vms1 to confer rapamycin resistance despite having normal expression and mitochondrial localization. Mutation of three highly conserved residues in the human Vms1 VIM also destroyed its ability to interact with VCP. VIM-deleted Vms1 also failed to interact with Npl4, suggesting that the Vms1-Npl4 interaction is mediated by Cdc48.

Fourth, it appears that the population of Cdc48-Npl4 complex that is Vms1-associated is distinct from that which is associated with Ufd1. We have shown that both Vms1 and Ufd1 co-purify with Cdc48 and Npl4, and protein-protein interaction screens have shown that both interact with various components of the ubiquitin/ proteasome system, including Ufd2 and Ufd3 (Jensen et al., 2009). In spite of this, Vms1 and Ufd1 do not co-purify in multiple experimental formats in our hands and there is no indication that Vms1 and Ufd1 interact in published datasets. Consistent with an important role in ERAD, protein interaction data suggest that Ufd1 interacts with Der1 (Jensen et al., 2009), an ER membrane protein that is a central component of the ERAD machinery (Vembar and Brodsky, 2008). In contrast, there is no indication of interaction of Vms1 with ER resident proteins and our data demonstrate mitochondrial localization of Vms1 under the conditions where the protein is most important for cell survival. The roles of Vms1 and Ufd1 in protein degradation are also distinct. The *vms1*Δ mutant has impaired Fzo1 degradation, but under identical conditions, has modestly accelerated degradation of CPY*, which is almost absent in a *ufd1-1* mutant. Genetically, both Cdc48 and Npl4 partially suppressed the *vms1*Δ mutant phenotype, but Ufd1 overexpression had no effect. Based on these combined data, we suggest that the Vms1-associated Cdc48-Npl4 complex promotes mitochondrial protein degradation, while the Ufd1-associated proportion is required for the well-documented role of Cdc48 in ER protein degradation (Figure S7E).

Fifth, Vms1 is required for normal ubiquitin-dependent protein degradation at mitochondria, specifically on the mitochondrial outer membrane. The best-characterized mitochondrial substrate of the ubiquitin/ proteasome system in yeast is the outer membrane protein Fzo1, and its degradation is impaired in the *vms1*Δ mutant. We suggest that Fzo1 is indicative of a broader impairment of ubiquitin-dependent protein degradation at the mitochondrial outer membrane and that impaired Fzo1 degradation is not a major cause of the *vms1*Δ mutant phenotypes we have observed. We, therefore, anticipate that the degradation of other proteins associated with the mitochondrial outer membrane will be found to be dependent on Vms1. Indeed, mitochondrial ubiquitin/ proteasome system-dependent protein degradation appears to be widely compromised in the *vms1*Δ mutant as evidenced by the altered accumulation of many poly-ubiquitinated proteins.

Sixth, loss of Vms1 increases cellular reliance on other, non-proteasomal modes of mitochondrial protein degradation. We observed enhanced mitophagy in the *vms1*Δ mutant relative to wild-type, which was confirmed by examination of the steady state levels of a series of proteins from different mitochondrial compartments. The other major mode of mitochondrial protein degradation is enacted by intrinsic mitochondrial proteases, including Oma1 and Yme1. In the absence of Vms1, both Oma1 and Yme1 become almost completely essential for glycerol growth. These two pieces of data are strongly suggestive of a role for Vms1 in mitochondrial protein degradation. The coordination of proteasomal protein degradation and mitophagy and their role in maintaining mitochondrial function, preventing ROS accumulation and cell death has been also observed by others (Takeda et al., 2010). The synthetic respiratory defect caused by loss of Vms1 and either Oma1 or Yme1, both of which reside in the mitochondrial inner membrane, raises an important question. Does

Vms1, and by extension the ubiquitin-proteasome system, participate in the degradation of internal mitochondrial proteins? In mammalian cells, the intrinsic mitochondrial inner membrane proteins, UCP-2 and UCP-3, have both recently been shown to have unusually short half-lives, which are dependent upon the cytosolic proteasome (Azzu and Brand, 2010; Azzu et al., 2010). The OSCP subunit of the mitochondrial Complex V ATP synthase has also shown to be ubiquitinated and degraded by the cytosolic proteasome (Margineantu et al., 2007). It is possible that a mitochondrial retrotranslocation system, analogous to that of the endoplasmic reticulum in ERAD, might extrude proteins for degradation in the cytosol.

Finally, the aberrant cellular physiology of the *vms1*Δ mutant suggests that the Vms1 protein is required for maintenance of mitochondrial function. The loss of Vms1 causes a marked time-dependent failure of mitochondrial respiration. Concurrently, we also observed an increase in oxidative stress and its damaging effects. Likely as a direct consequence, the *vms1*Δ mutant exhibits progressively more pronounced cell death in static culture. Interestingly, these phenotypes are strikingly similar to that observed for the S565G mutant of Cdc48 (Braun et al., 2006; Madeo et al., 1997), which fails to stably interact with Vms1. Therefore, two independent genetic manipulations, mutation of Cdc48 and deletion of Vms1, that prevent the Vms1-dependent regulation of Cdc48 both cause cell death with similar mitochondrial sequellae. The importance of mitochondrial protein quality control for mitochondrial function and healthy lifespan has been recently emphasized by studies of the mitochondrial matrix Lon protease (Luce and Osiewacz, 2009).

Based on these genetic and biochemical connections, we propose a model wherein mitochondrial stress causes the recruitment of a subpopulation of Cdc48 and Npl4 to mitochondria through their interaction with Vms1 (Figure S7E). We suggest that the Vms1-dependent translocation to mitochondria enables Cdc48 and its cofactor Npl4 to perform a function on mitochondria that is similar to its function in ERAD. In the absence of Vms1, damaged, misfolded and ubiquitinated proteins accumulate causing progressive mitochondrial dysfunction and eventually cell death.

These data and the high degree of conservation throughout eukaryotes suggest that Vms1 performs similar functions in higher eukaryotes. We propose that Vms1 is a component of an evolutionarily conserved system for maintaining mitochondrial function through protein quality control. In its absence, progressive mitochondrial dysfunction causes shortened lifespan as observed in yeast and worms. Due to the central role for mitochondrial dysfunction in age-related human diseases, including neurodegenerative diseases, we consider it likely that alterations in Vms1 expression, activity or associations would impact the incidence of such pathologies. Indeed, mutations in VCP, the human ortholog of Cdc48, cause progressive muscle weakness and frontotemporal dementia (Watts et al., 2004; Weihl et al., 2009). Of more direct interest, a locus conferring susceptibility to Alzheimers disease has been mapped to human chromosome 2q (Holmans et al., 2005), with a second study mapping susceptibility to the immediate vicinity of the human *VMS1* ortholog (Scott et al., 2003). It will be important to define whether these susceptibility loci are related to alterations in Vms1 function. A more detailed understanding of the Vms1 system could aid in understanding the mitochondrial etiology of disease and the cellular systems to prevent it.

Experimental Procedures

Fluorescence microscopy

The *vms1*Δ strain was transformed with both pVMS1-GFP (or pVMS1 deletion mutant-GFP) and pMito-RFP plasmids. To test the effect of rapamycin treatment on Vms1 localization, strains were grown to mid-log phase at 30°C in SD medium lacking both uracil and leucine and treated with vehicle or rapamycin (200ng/ ml) for 3 h, and imaged using a

Zeiss Axioplan 2 Imaging microscope (Carl Zeiss) as described (Kondo-Okamoto et al., 2003). Hydrogen peroxide (3mM for either 90 minutes (Vms1 localization) or 3 hours (Cdc48 localization)), antimycin A, oligomycin, CCCP, FCCP (10 μM for 3 hours), and stationary phase experiments were done otherwise identically. For Cdc48 and Npl4 localization, the WT and *vms1*Δ strains expressing C-terminally GFP-tagged Cdc48 or Npl4 from the native *CDC48* or *NPL4* locus were treated as above.

Mitochondrial localization was quantified using Image J software in a blinded manner. The GFP signal intensity that overlapped with mito-RFP (designated mitochondria) was quantified. Average total cellular GFP signal intensity was also quantified for each cell. Mitochondrial localization was expressed as a ratio of mitochondrially co-localized GFP and total cellular GFP.

Yeast Vms1 Tandem Affinity Purification (TAP) purification

TAP purification was performed as previously described (Puig et al., 2001). The *vms1*Δ strain, transformed with C-terminally TAP-tagged Vms1 construct under the native *VMS1* promoter, was grown to late log phase and harvested. Cleared lysates were generated and incubated with IgG-agarose beads for 4 h at 4°C, washed, and treated with TEV protease for 2 h at 17°C. The TEV cleavage eluate was then incubated with calmodulin beads for 2 h at 4°C and the final eluates were obtained with EGTA elution. Eluates were then analyzed by SDS-PAGE and Coomassie Blue staining. The unique bands detected were identified by LC-MS-MS. For negative control, JRY472 strain transformed with empty vector was analyzed in parallel.

Fzo1 and CPY* degradation assay

WT, *vms1*Δ, and *ufd1-1* strains transformed with either pRS414-Fzo1-HA or pRS414-CPY*-HA construct were grown to log phase and treated with 0.1mg/ ml cycloheximide. For each time point, the same number of cells was harvested, washed, and lysed for each culture as described (Kushnirov, 2000). Each lysate was then subjected to western blotting using anti-HA and porin antibodies. The levels of Fzo1-HA and CPY*-HA were normalized to that of porin and Pgk1 in the same sample, respectively. Note that cycloheximide causes Vms1 translocation to mitochondria.

Tandem Affinity Purification (TAP) and Immunoprecipitation from Mammalian Cells

C2C12 cells stably expressing an empty integration cassette or mouse Vms1 (NM_026187.4) with a C-terminal Flag-HA tag (acg gat cca gcc gcc gac tac aag gac gac gat gac aaa gcc ctg gcc tac cca tac gat gtg cca gat tac gct) were grown to 90% confluency. Cells were lysed in buffer containing 40 mM Hepes, 100 mM NaCl, 5 mM $Na_4P_2O_7$, 5 mM 2-glycerophosphate, 10 mM NaF, 20 μM $ZnCl_2$, 0.02% Igepal 630, and EDTA-free Complete Protease Inhibitor mix (Roche), at pH 7.5. Lysates were clarified by centrifugation for 10 min at 16,000 × g. Vms1-Flag-HA was immunoprecipitated from supernatants by incubation for 2 h with agarose beads pre-conjugated to either anti-Flag (Sigma, F2426) or anti-HA antibody (Sigma, A2095). For the tandem affinity purification of Vms1, the clarified lysates from 4 × 10 cm dishes were pooled and subjected to immunoprecipitation by Flag, and then washed 4x with Wash Buffer (Lysis Buffer but with 120 mM NaCl and 0.1% Igepal-630). Washed Vms1-Flag-HA was eluted by incubation with 250 μg/ ml 3X flag peptide for 45 min, on ice and then re-purified by HA, washed 2x with Wash Buffer, and eluted by incubation with 250 μg/ ml HA peptide for 45 min at RT. Immunoprecipitates were subjected to SDS-PAGE and the resultant gel was silver stained using the Pierce Silver Stain for Mass Spectrometry (24600). To test whether an intact VIM was required for co-immunoprecipitation of Vms1-Flag-HA and p97, complexes were pulled-down by Flag and eluted by heating with 1.5X Laemmli's Buffer. Clarified lysates, supernatants, and eluates

were immunoblotted for Vms1 using an affinity purified anti-mouse Vms1 antibody that was generated by Cell Signaling Technology by immunizing rabbits. VCP/ p97 antibody from mouse was from Abcam (ab11433).

Supplementary Material

Refer to Web version on PubMed Central for supplementary material.

Acknowledgments

We wish to thank members of the Rutter laboratory as well as David Stillman, Janet Shaw, Dennis Winge and Jerry Kaplan and their laboratories for technical support and helpful discussions. We thank Janet Shaw for the Fzo1-HA and mito-RFP constructs and fluorescence microscopy; the Stillman lab for plasmids and yeast strains; the Winge lab for antibodies, protocols and oxygen consumption assays; William Lenarz for the CPY* plasmid. We also thank members of the Ashrafi laboratory for helpful discussions and technical assistance, members of the Kenyon lab for help with lifespan analysis software, Shohei Mitani and the National Bioresource Project for strains and Stefan Taubert for reagents. This work was supported by NIH grants DK071962 and GM087346 (to J.R.), DK070149 (to K.A.), GM75061 (to J.L.B.), grants from the Israel Science Foundation, the USA-Israel Binational Science Foundation, and the Israel Cancer Association (to M.H.G.) and FWF grant S-9304-B05 (to F.M). E.B.T. was supported by an American Heart Association Postdoctoral Fellowship 09POST2110034.

References Cited

Andreoli C, Prokisch H, Hortnagel K, Mueller JC, Munsterkotter M, Scharfe C, Meitinger T. MitoP2, an integrated database on mitochondrial proteins in yeast and man. Nucleic Acids Res. 2004; 32:D459–462. [PubMed: 14681457]

Azzu V, Brand MD. Degradation of an intramitochondrial protein by the cytosolic proteasome. J Cell Sci. 2010; 123:578–585. [PubMed: 20103532]

Azzu V, Mookerjee SA, Brand MD. Rapid turnover of mitochondrial uncoupling protein 3. Biochem J. 2010; 426:13–17. [PubMed: 19954423]

Bays NW, Hampton RY. Cdc48-Ufd1-Npl4: stuck in the middle with Ub. Curr Biol. 2002; 12:R366–371. [PubMed: 12015140]

Bestwick M, Khalimonchuk O, Pierrel F, Winge DR. The role of Coa2 in hemylation of yeast Cox1 revealed by its genetic interaction with Cox10. Mol Cell Biol. 2010; 30:172–185. [PubMed: 19841065]

Braun RJ, Zischka H, Madeo F, Eisenberg T, Wissing S, Buttner S, Engelhardt SM, Buringer D, Ueffing M. Crucial mitochondrial impairment upon CDC48 mutation in apoptotic yeast. J Biol Chem. 2006; 281:25757–25767. [PubMed: 16822868]

Cohen MM, Leboucher GP, Livnat-Levanon N, Glickman MH, Weissman AM. Ubiquitin-proteasome-dependent degradation of a mitofusin, a critical regulator of mitochondrial fusion. Mol Biol Cell. 2008; 19:2457–2464. [PubMed: 18353967]

Ehses S, Raschke I, Mancuso G, Bernacchia A, Geimer S, Tondera D, Martinou JC, Westermann B, Rugarli EI, Langer T. Regulation of OPA1 processing and mitochondrial fusion by m-AAA protease isoenzymes and OMA1. J Cell Biol. 2009; 187:1023–1036. [PubMed: 20038678]

Elstner M, Andreoli C, Ahting U, Tetko I, Klopstock T, Meitinger T, Prokisch H. MitoP2: an integrative tool for the analysis of the mitochondrial proteome. Mol Biotechnol. 2008; 40:306–315. [PubMed: 18780189]

Escobar-Henriques M, Westermann B, Langer T. Regulation of mitochondrial fusion by the F-box protein Mdm30 involves proteasome-independent turnover of Fzo1. J Cell Biol. 2006; 173:645–650. [PubMed: 16735578]

Fabrizio P, Pozza F, Pletcher SD, Gendron CM, Longo VD. Regulation of longevity and stress resistance by Sch9 in yeast. Science. 2001; 292:288–290. [PubMed: 11292860]

Fritz S, Weinbach N, Westermann B. Mdm30 is an F-box protein required for maintenance of fusion-competent mitochondria in yeast. Mol Biol Cell. 2003; 14:2303–2313. [PubMed: 12808031]

Ghaemmaghami S, Huh WK, Bower K, Howson RW, Belle A, Dephoure N, O'Shea EK, Weissman JS. Global analysis of protein expression in yeast. Nature. 2003; 425:737–741. [PubMed: 14562106]

Hao HX, Khalimonchuk O, Schraders M, Dephoure N, Bayley JP, Kunst H, Devilee P, Cremers CW, Schiffman JD, Bentz BG, et al. SDH5, a gene required for flavination of succinate dehydrogenase, is mutated in paraganglioma. Science. 2009; 325:1139–1142. [PubMed: 19628817]

Hao HX, Rutter J. Revealing human disease genes through analysis of the yeast mitochondrial proteome. Cell Cycle. 2009; 8:4007–4008. [PubMed: 19949294]

Head B, Griparic L, Amiri M, Gandre-Babbe S, van der Bliek AM. Inducible proteolytic inactivation of OPA1 mediated by the OMA1 protease in mammalian cells. J Cell Biol. 2009; 187:959–966. [PubMed: 20038677]

Holmans P, Hamshere M, Hollingworth P, Rice F, Tunstall N, Jones S, Moore P, Wavrant DeVrieze F, Myers A, Crook R, et al. Genome screen for loci influencing age at onset and rate of decline in late onset Alzheimer's disease. Am J Med Genet B Neuropsychiatr Genet. 2005; 135B:24–32. [PubMed: 15729734]

Hu J, Barr MM. ATP-2 interacts with the PLAT domain of LOV-1 and is involved in Caenorhabditis elegans polycystin signaling. Mol Biol Cell. 2005; 16:458–469. [PubMed: 15563610]

Jensen LJ, Kuhn M, Stark M, Chaffron S, Creevey C, Muller J, Doerks T, Julien P, Roth A, Simonovic M, et al. STRING 8--a global view on proteins and their functional interactions in 630 organisms. Nucleic Acids Res. 2009; 37:D412–416. [PubMed: 18940858]

Jentsch S, Rumpf S. Cdc48 (p97): a “molecular gearbox” in the ubiquitin pathway? Trends Biochem Sci. 2007; 32:6–11. [PubMed: 17142044]

Kass J, Jacob TC, Kim P, Kaplan JM. The EGL-3 proprotein convertase regulates mechanosensory responses of Caenorhabditis elegans. J Neurosci. 2001; 21:9265–9272. [PubMed: 11717360]

Kissova I, Deffieu M, Samokhvalov V, Velours G, Bessoule JJ, Manon S, Camougrand N. Lipid oxidation and autophagy in yeast. Free Radic Biol Med. 2006; 41:1655–1661. [PubMed: 17145553]

Koppen M, Langer T. Protein degradation within mitochondria: versatile activities of AAA proteases and other peptidases. Crit Rev Biochem Mol Biol. 2007; 42:221–242. [PubMed: 17562452]

Livnat-Levanon N, Glickman MH. Ubiquitin Proteasome System and Mitochondria - Reciprocity. Biochemica Biophysica Acta. 2010 In press.

Luce K, Osiewacz HD. Increasing organismal healthspan by enhancing mitochondrial protein quality control. Nat Cell Biol. 2009; 11:852–858. [PubMed: 19543272]

Madeo F, Frohlich E, Frohlich KU. A yeast mutant showing diagnostic markers of early and late apoptosis. J Cell Biol. 1997; 139:729–734. [PubMed: 9348289]

Margineantu DH, Emerson CB, Diaz D, Hockenbery DM. Hsp90 inhibition decreases mitochondrial protein turnover. PLoS ONE. 2007; 2:e1066. [PubMed: 17957250]

Meisinger C, Sickmann A, Pfanner N. The mitochondrial proteome: from inventory to function. Cell. 2008; 134:22–24. [PubMed: 18614007]

Murphy CT, McCarroll SA, Bargmann CI, Fraser A, Kamath RS, Ahringer J, Li H, Kenyon C. Genes that act downstream of DAF-16 to influence the lifespan of Caenorhabditis elegans. Nature. 2003; 424:277–283. [PubMed: 12845331]

Nogae I, Johnston M. Isolation and characterization of the ZWF1 gene of Saccharomyces cerevisiae, encoding glucose-6-phosphate dehydrogenase. Gene. 1990; 96:161–169. [PubMed: 2269430]

Oh SW, Mukhopadhyay A, Dixit BL, Raha T, Green MR, Tissenbaum HA. Identification of direct DAF-16 targets controlling longevity, metabolism and diapause by chromatin immunoprecipitation. Nat Genet. 2006; 38:251–257. [PubMed: 16380712]

Okamoto K, Kondo-Okamoto N, Ohsumi Y. Mitochondria-anchored receptor Atg32 mediates degradation of mitochondria via selective autophagy. Dev Cell. 2009; 17:87–97. [PubMed: 19619494]

Outten CE, Culotta VC. A novel NADH kinase is the mitochondrial source of NADPH in Saccharomyces cerevisiae. Embo J. 2003; 22:2015–2024. [PubMed: 12727869]

Pagliarini DJ, Calvo SE, Chang B, Sheth SA, Vafai SB, Ong SE, Walford GA, Sugiana C, Boneh A, Chen WK, et al. A mitochondrial protein compendium elucidates complex I disease biology. Cell. 2008; 134:112–123. [PubMed: 18614015]

Petit P, Glab N, Marie D, Kieffer H, Metezeau P. Discrimination of respiratory dysfunction in yeast mutants by confocal microscopy, image, and flow cytometry. Cytometry. 1996; 23:28–38. [PubMed: 14650438]

Priault M, Salin B, Schaeffer J, Vallette FM, di Rago JP, Martinou JC. Impairing the bioenergetic status and the biogenesis of mitochondria triggers mitophagy in yeast. Cell Death Differ. 2005; 12:1613–1621. [PubMed: 15947785]

Raasi S, Wolf DH. Ubiquitin receptors and ERAD: a network of pathways to the proteasome. Semin Cell Dev Biol. 2007; 18:780–791. [PubMed: 17942349]

Richly H, Rape M, Braun S, Rumpf S, Hoege C, Jentsch S. A series of ubiquitin binding factors connects CDC48/p97 to substrate multiubiquitylation and proteasomal targeting. Cell. 2005; 120:73–84. [PubMed: 15652483]

Rodriguez-Manzaneque MT, Ros J, Cabiscol E, Sorribas A, Herrero E. Grx5 glutaredoxin plays a central role in protection against protein oxidative damage in Saccharomyces cerevisiae. Mol Cell Biol. 1999; 19:8180–8190. [PubMed: 10567543]

Scott WK, Hauser ER, Schmechel DE, Welsh-Bohmer KA, Small GW, Roses AD, Saunders AM, Gilbert JR, Vance JM, Haines JL, et al. Ordered-subsets linkage analysis detects novel Alzheimer disease loci on chromosomes 2q34 and 15q22. Am J Hum Genet. 2003; 73:1041–1051. [PubMed: 14564669]

Sickmann A, Reinders J, Wagner Y, Joppich C, Zahedi R, Meyer HE, Schonfisch B, Perschil I, Chacinska A, Guiard B, et al. The proteome of Saccharomyces cerevisiae mitochondria. Proc Natl Acad Sci U S A. 2003; 100:13207–13212. Epub 12003 Oct 13223. [PubMed: 14576278]

Takeda K, Yoshida T, Kikuchi S, Nagao K, Kokubu A, Pluskal T, Villar-Briones A, Nakamura T, Yanagida M. Synergistic roles of the proteasome and autophagy for mitochondrial maintenance and chronological lifespan in fission yeast. Proc Natl Acad Sci U S A. 2010; 107:3540–3545. [PubMed: 20133687]

Tatsuta T. Protein quality control in mitochondria. J Biochem. 2009; 146:455–461. [PubMed: 19666648]

Vembar SS, Brodsky JL. One step at a time: endoplasmic reticulum-associated degradation. Nat Rev Mol Cell Biol. 2008; 9:944–957. [PubMed: 19002207]

Wallace DC. A mitochondrial paradigm of metabolic and degenerative diseases, aging, and cancer: a dawn for evolutionary medicine. Annu Rev Genet. 2005; 39:359–407. [PubMed: 16285865]

Watts GD, Wymer J, Kovach MJ, Mehta SG, Mumm S, Darvish D, Pestronk A, Whyte MP, Kimonis VE. Inclusion body myopathy associated with Paget disease of bone and frontotemporal dementia is caused by mutant valosin-containing protein. Nat Genet. 2004; 36:377–381. [PubMed: 15034582]

Weihl CC, Pestronk A, Kimonis VE. Valosin-containing protein disease: inclusion body myopathy with Paget's disease of the bone and fronto-temporal dementia. Neuromuscul Disord. 2009; 19:308–315. [PubMed: 19380227]

Werner-Washburne M, Braun E, Johnston GC, Singer RA. Stationary phase in the yeast Saccharomyces cerevisiae. Microbiol Rev. 1993; 57:383–401. [PubMed: 8393130]

Ye Y. Diverse functions with a common regulator: ubiquitin takes command of an AAA ATPase. J Struct Biol. 2006; 156:29–40. [PubMed: 16529947]

Yeung HO, Kloppsteck P, Niwa H, Isaacson RL, Matthews S, Zhang X, Freemont PS. Insights into adaptor binding to the AAA protein p97. Biochem Soc Trans. 2008; 36:62–67. [PubMed: 18208387]

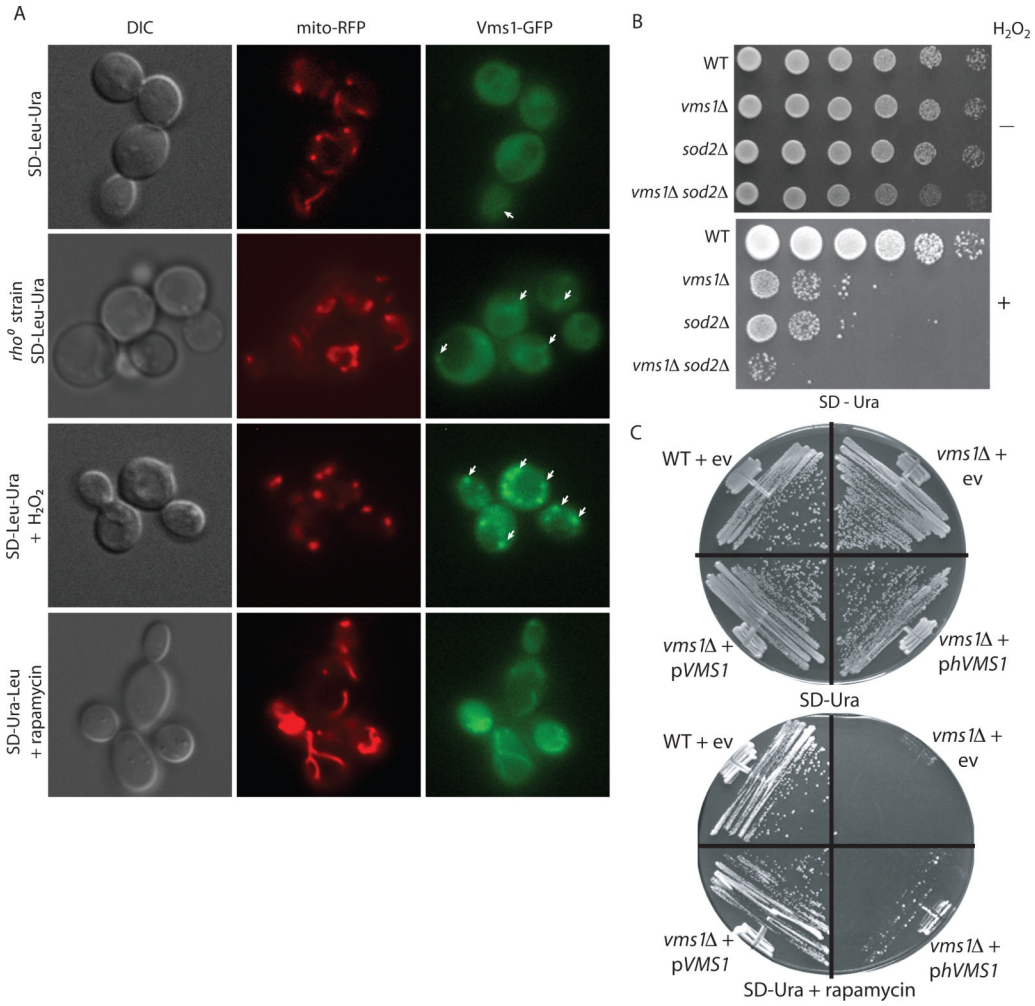

Figure 1. Vms1 exhibits stress-responsive mitochondrial translocation and loss of Vms1 causes hypersensitivity to hydrogen peroxide and rapamycin

(A) The *vms1*Δ strain containing both a plasmid expressing mito-RFP (a fusion of the *N. crassa* Su9 presequence to RFP) and a plasmid expressing Vms1-GFP under the native *VMS1* promoter was grown in SD-Ura-Leu medium. Upon reaching mid-log phase, the culture was either treated with vehicle (top) or with compounds as indicated and subjected to fluorescence microscopy. The 2nd row shows representative images of Vms1-GFP localization in an *vms1*Δ *rho*^{o} strain (lacking the mitochondrial genome) in log phase. The field shown in the top image was selected to show the weak mitochondrial localization of Vms1-GFP in the absence of stressor in a small percentage of cells (indicated with an arrow). Representative images are shown. (B) WT, *vms1*Δ, *sod2*Δ, and *vms1*Δ *sod2*Δ strains were grown to saturation in SD-Ura. Serial 5-fold dilutions of each culture were spotted on both SD-Ura (top) and SD-Ura + 3mM hydrogen peroxide (bottom) plates and grown at 30°C for 2 days. (C) WT and *vms1*Δ strains were transformed with empty vector (ev), a plasmid containing the yeast *VMS1* gene (pVMS1), or a plasmid containing the human *VMS1* gene under the control of the yeast GPD promoter (pHsVMS1). Each strain was streaked on an SD-Ura plate without (top) or with 30ng/ ml rapamycin (bottom) and grown at 30°C for 2 days (top) or 5 days (bottom).

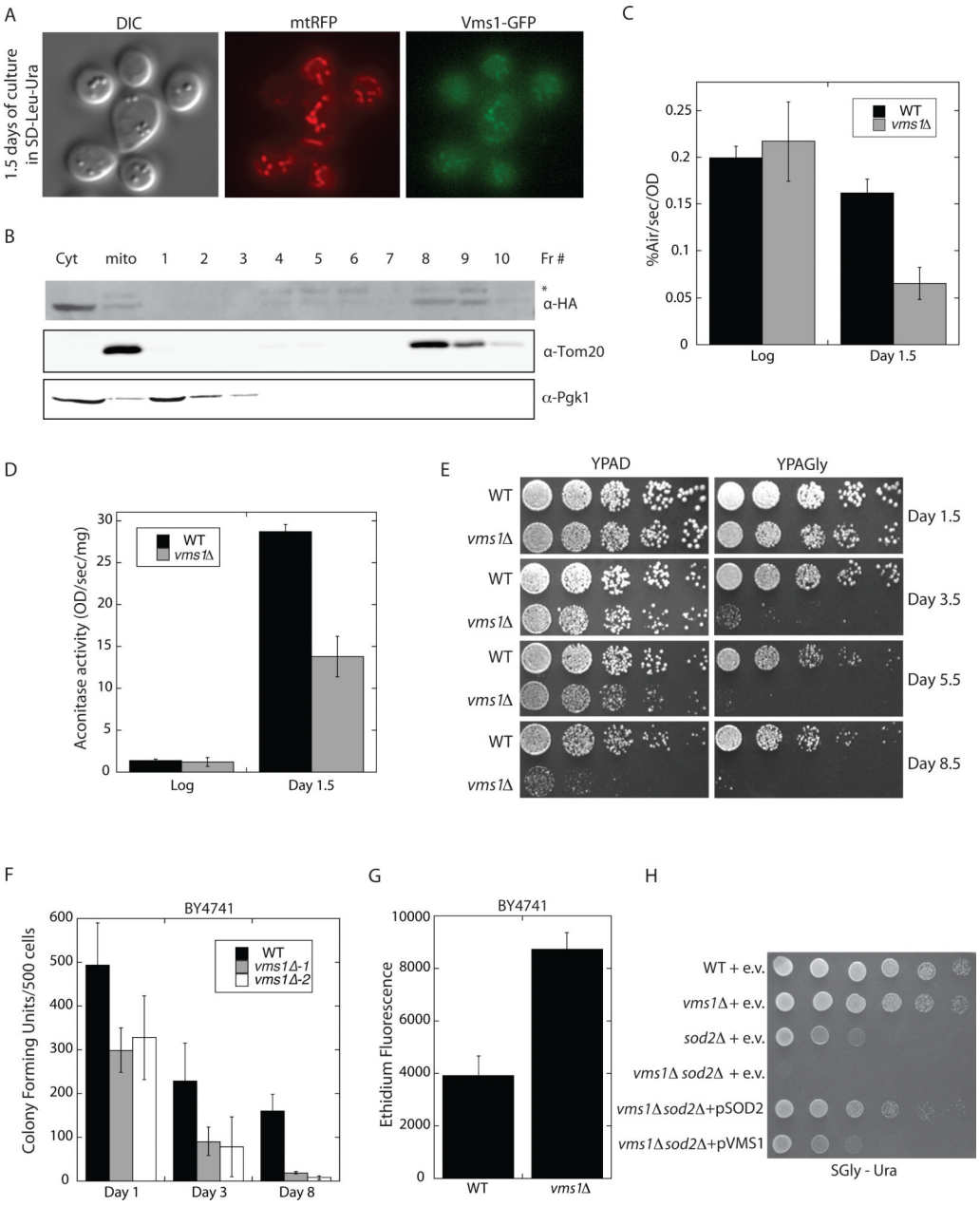

Figure 2. Deletion of *VMS1* induces mitochondrial dysfunction

(A) The *vms1*Δ strain containing plasmids expressing mito-RFP and Vms1-GFP was grown in SD-Leu-Ura for 1.5 days and subjected to fluorescence imaging. (B) The *vms1*Δ strain containing a plasmid expressing C-terminally HA-tagged Vms1 was grown for 1.5 days and subjected to differential centrifugation. The mitochondria enriched fraction (mito) was then fractionated on a sucrose cushion and subjected to SDS-PAGE followed by western blot. Tom20 and Pgk1 were used as mitochondrial and cytop lasmic markers, respectively. (C and D) WT and *vms1*Δ strains grown in SD medium were harvested at either log phase or at day 1.5 of culture and were subjected to oxygen consumption assay (C) and aconitase activity assay (D). Mean ± s.d of three independent cultures is shown. (E) WT and *vms1*Δ strains in the W303 background, grown in synthetic complete glucose (SD) media for 1.5, 3.5, 5.5, or 8.5 days, were 5-fold serially diluted and equivalent cell numbers of each strain were spotted

on both YPAD and YPAGlycerol plates and grown at 30°C. (F) WT and two independent *vms1*Δ strains in the BY4741 background were grown in synthetic complete glucose (SD) media for 1, 3, or 8 days. 500 cells from each culture were plated on YPAD and grown at 30°C for determination of colony formation. Colony forming units were determined for at least three independent cultures per strain and mean ± s.d. is shown. (G) WT and *vms1*Δ strains in the BY4741 background were grown in synthetic complete glucose (SD) media for 4 days and stained with dihydroethidium. Ethidium fluorescence was determined by FACS analysis for each strain. For each strain, three independent cultures were tested and mean ± s.d. is shown. (H) WT, *vms1*Δ, *sod2*Δ, and *vms1*Δ *sod2*Δ strains were transformed with empty vector (ev), a plasmid containing the *SOD2* gene (pSOD2) or a plasmid containing the *VMS1* gene (pVMS1). Each strain was grown to saturation in SD-Ura media. Serial 5-fold dilutions of each culture were then spotted on an SGlycerol-Ura plate, and grown at 30°C.

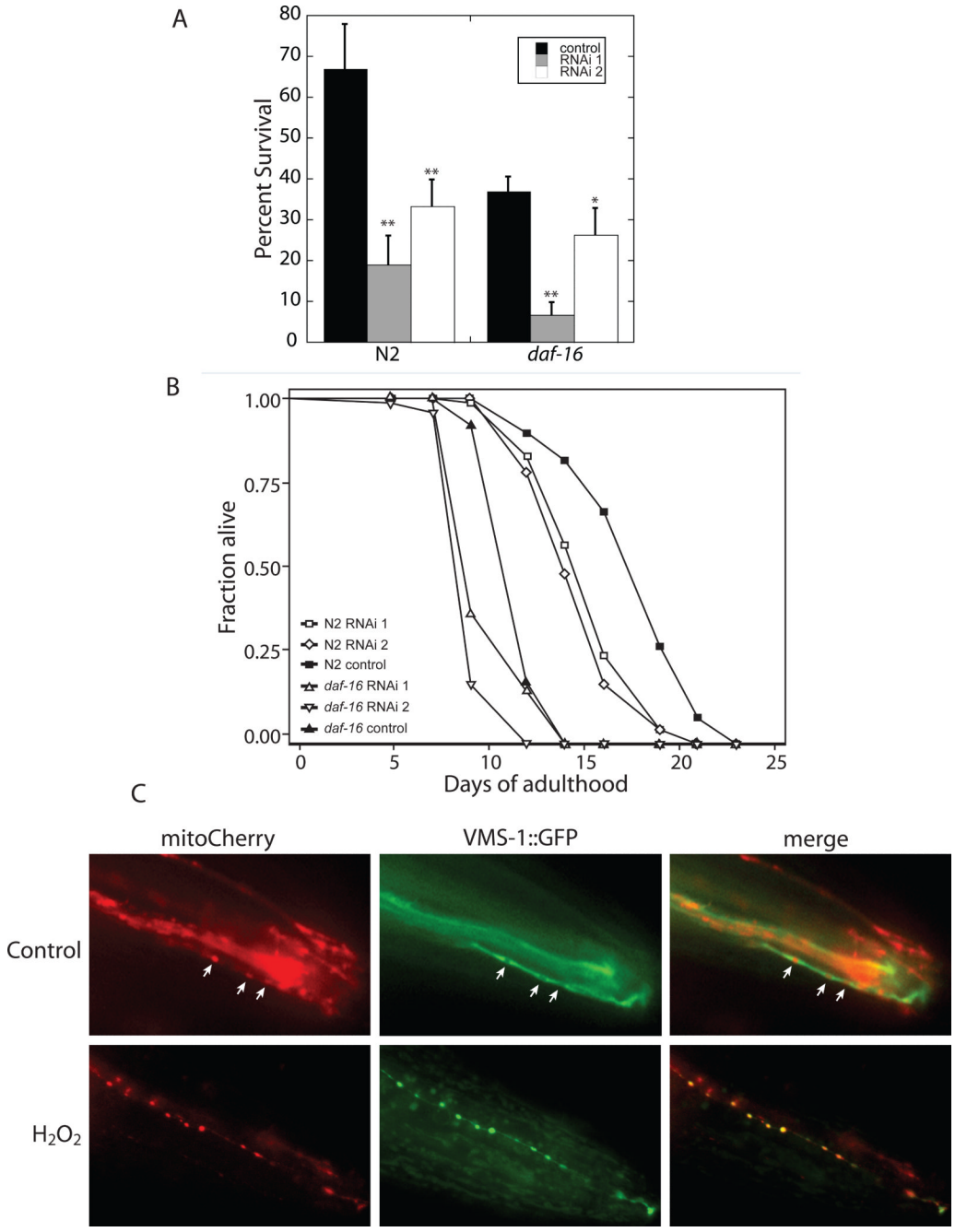

Figure 3. *C. elegans vms-1* is required for wild-type lifespan and hydrogen peroxide resistance

(A) Wild-type (N2) or *daf-16* mutant worms were grown to the first day of egglaying on bacteria expressing vector control or either of two independent *vms-1* RNAi constructs, and their survival was scored after 5 h in 20mM H_2O_2 at room temperature. Results shown are the average ± s.d. of three replicate experiments comprised of 100 animals each. * $p<0.05$ and ** $p<0.01$. (B) Wild-type (N2) or *daf-16* mutant worms grown as in (A) were assayed for lifespan. Mean lifespans were as follows: wild type on vector control was 18.0 ± 0.1d, wild type on RNAi 1 was 15.5 ± 0.2 d ($p<0.0001$), wild type on RNAi 2 was 15.0 ± 0.2 d ($p<0.0001$), *daf-16* on vector control was 12.1 ± 0.1 d, *daf-16* on RNAi 1 was 10.3 ± 0.1 d ($p<0.0001$), and *daf-16* on RNAi 2 was 9.3 ± 0.1d ($p<0.0001$). p values reflect statistical

significance of each RNAi treatment compared to vector control for each strain. (C) Subcellular localization of VMS-1::GFP in dendritic processes of amphid neurons was imaged in worms co-expressing *Pvms-1*::*VMS-1::GFP* and the mito-mCherry mitochondrial marker (*Pegl-3::DIC-1::mCherry*). Worms were treated for 1 h in either M9 as a control (top) or 200mM H_2O_2 dissolved in M9 (bottom). Representative images for each population are shown. Three sites of mito-mCherry localization and VMS-1::GFP exclusion in the control images are indicated with arrows.

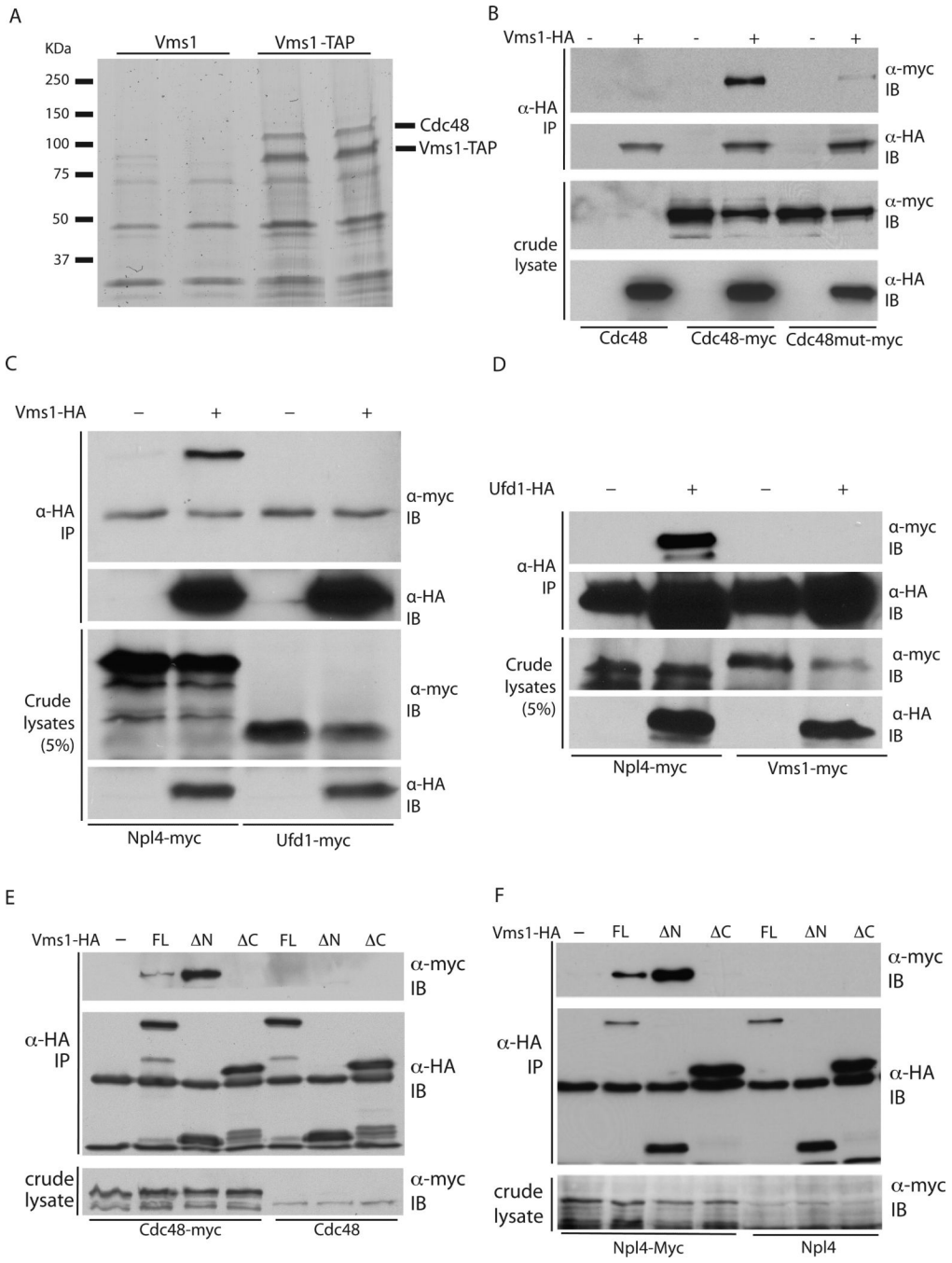

Figure 4. Vms1 constitutively interacts with Cdc48 and Npl4

(A) Strains expressing either untaggedor TAP-tagged Vms1 under the native *VMS1* promoter were grown to late log phase and subjected to TAP purification. The final eluates from each of two independent purifications for each strain were analyzed by SDS-PAGE and Coomassie staining. The major unique bands from the TAP-tagged Vms1 purification were identified by mass spectrometry as Cdc48 and Vms1-TAP as indicated. (B) WT, *vms1*Δ, *cdc48*Δ, and *vms*Δ *cdc48*Δ strains bearing plasmids expressing either Vms1 or Vms1-HA and Cdc48, Cdc48-myc, or Cdc48(S565G)-myc were grown to late log phase and subjected to immunoprecipitation with anti-HA antibody. Immunoblots of crude lysates and immunoprecipitates were developed with the indicated antibodies. (C) The *vms1*Δ, *vms1*Δ

*npl4*Δ, *ufd1*Δ, and *vms1*Δ *ufd1*Δ strains containing plasmids expressing either Vms1 or Vms1-HA and either Npl4-myc or Ufd1-myc were grown to late log phase and subjected to immunoprecipitation and immunoblot as in (B). (D) The *ufd1*Δ, *ufd1*Δ *npl4*Δ, *vms1*Δ, and *ufd1*Δ *vms1*Δ strains containing plasmids expressing either Ufd1 or Ufd1-HA and either Npl4-myc or Vms1-myc were analyzed as in (B). (E) The *vms1*Δ strain containing plasmids expressing either untagged full-length (-) or HA-tagged full-length (FL), C-terminus-only (ΔN) or N-terminus-only (ΔC) Vms1 deletion mutants and either untagged or myc-tagged Cdc48 were analyzed as in (B). (F) The *vms1*Δ strain containing plasmids expressing either untagged full-length (-) or HA-tagged full-length (FL), C-terminus-only (ΔN) or N-terminus-only (ΔC) Vms1 deletion mutants and either untagged or myc-tagged Npl4 were analyzed as in (B).

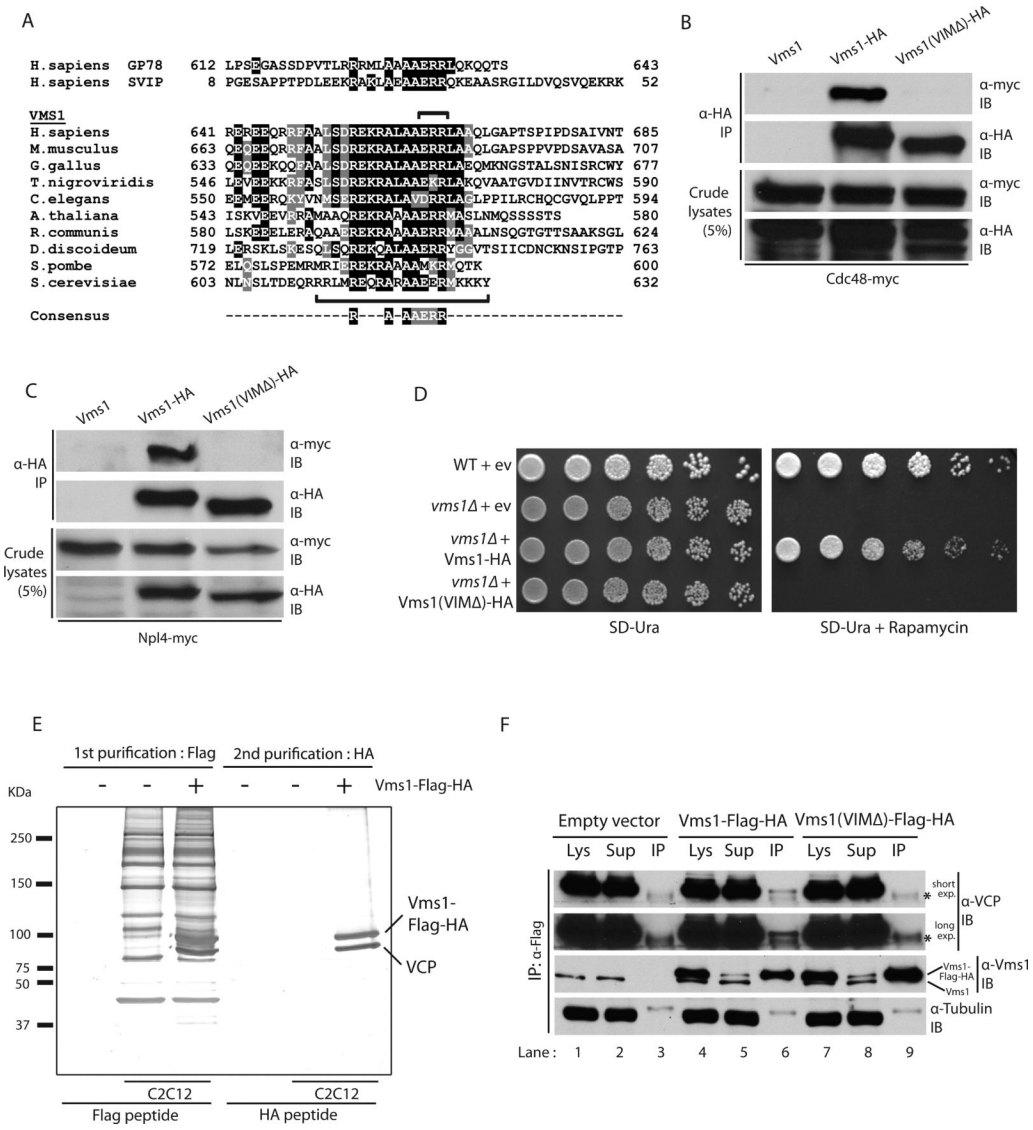

Figure 5. Vms1 interacts with Cdc48/Npl4 through a VIM and this interaction is required for Vms1 function

(A) Sequence alignment showing the VCP Interacting Motif (VIM) from known VCP interacting proteins and *VMS1* orthologs. The amino acids mutated in human Vms1 for use in (F) are bracketed above the sequence. The amino acids deleted in yeast Vms1 for use in (B, C, D) are bracketed below the sequence. (B) The *cdc48*Δ *vms1*Δ strain containing plasmids expressing either Vms1, Vms1-HA, or Vms1 (VIMΔ)-HA and either Cdc48 or Cdc48-myc was grown to late log phase and subjected to immunoprecipitation using anti-HA antibody. Immunoblots of crude lysates and immunoprecipitates were developed with the indicated antibodies. (C) The *vms1*Δ *npl4*Δ strain containing plasmids expressing either Vms1, Vms1-HA or Vms1 (VIMΔ)-HA and either Npl4 or Npl4-myc was grown to late log phase and analyzed as in (B). (D) WT and *vms1*Δ strains transformed with empty vector or centromeric plasmids expressing Vms-HA or Vms1 (VIMΔ)-HA from the endogenous *VMS1* promoter were grown to saturation in SD-Ura medium. 5-fold serial dilution of equivalent cell numbers were then spotted on both SD-Ura (left) and SD-Ura + 20ng/ ml rapamycin (right) plates and grown at 30°C. (E) C2C12 cells stably expressing either C-terminally Flag-HA tagged VMS1 (+) or empty vector (-) were harvested and subjected to

two-step affinity purification: immunoprecipitation with anti-Flag antibody and eluted with triple-Flag peptide; and immunoprecipitation with anti-HA antibody and eluted with HA peptide. Equivalent amounts of eluates were separated by SDS-PAGE and subjected to silver staining. (F) Control C2C12 cells or cells stably expressing either mouse VMS1-Flag-HA or VMS1(VIMΔ)-Flag-HA wherein VIM residues 684-686 (ERR—as indicated in (A)) were mutated to AAA were harvested and the lysates were subjected to immunoprecipitation with anti-Flag antibody. Lysates (Lys), immunodepleted supernatants (Sup), and immunoprecipitates (IP) were analyzed by western blot for VMS1 and VCP. VMS1-Flag-HA and VMS1(VIMΔ)-Flag-HA were expressed at and immunoprecipitated in equal amounts (upper band; lower band is endogenous VMS1). The asterisk indicates a non-specific band. Tubulin was used as a loading control for lysates and immunodepleted supernatants.

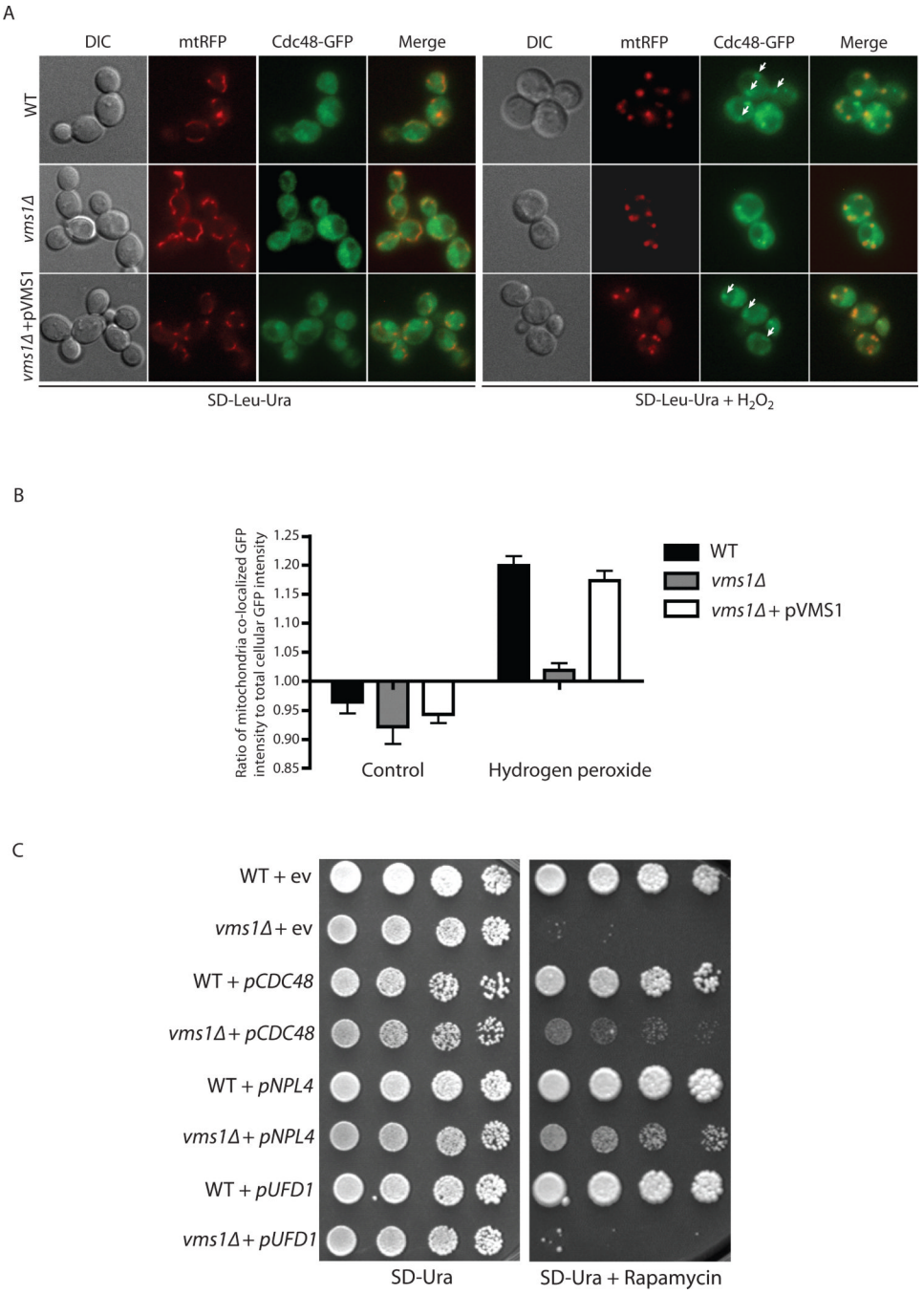

Figure 6. Vms1 is required for the mitochondrial translocation of Cdc48

(A) WT and *vms1*Δ strains expressing a functional Cdc48-GFP fusion protein from the native *CDC48* locus were transformed with mito-RFP plasmid and either empty vector or centromeric pVMS1-HA and cultured in SD-Leu-Ura at 30°C. Upon reaching mid-log phase, the culture was treated with either vehicle (left) or 3mM hydrogen peroxide for 3 hours (right) and imaged. Representative images are shown. (B) Ratio of mitochondria (mito-RFP) co-localized Cdc48-GFP to total cellular Cdc48-GFP signal (± s.e.m) is graphed for each strain and condition from (A). At least 50 blindly selected cells were analyzed for each strain and condition. (C) WT and *vms1*Δ strains transformed with either pRS426 (ev), pRS426-*CDC48*, pRS426-*NPL4*, or pRS426-*UFD1* were grown to saturation in SD-Ura

medium and serial 5-fold dilutions were spotted on both SD-Ura (left) and SD-Ura + 20ng/ml rapamycin (right) plates and grown at 30°C.

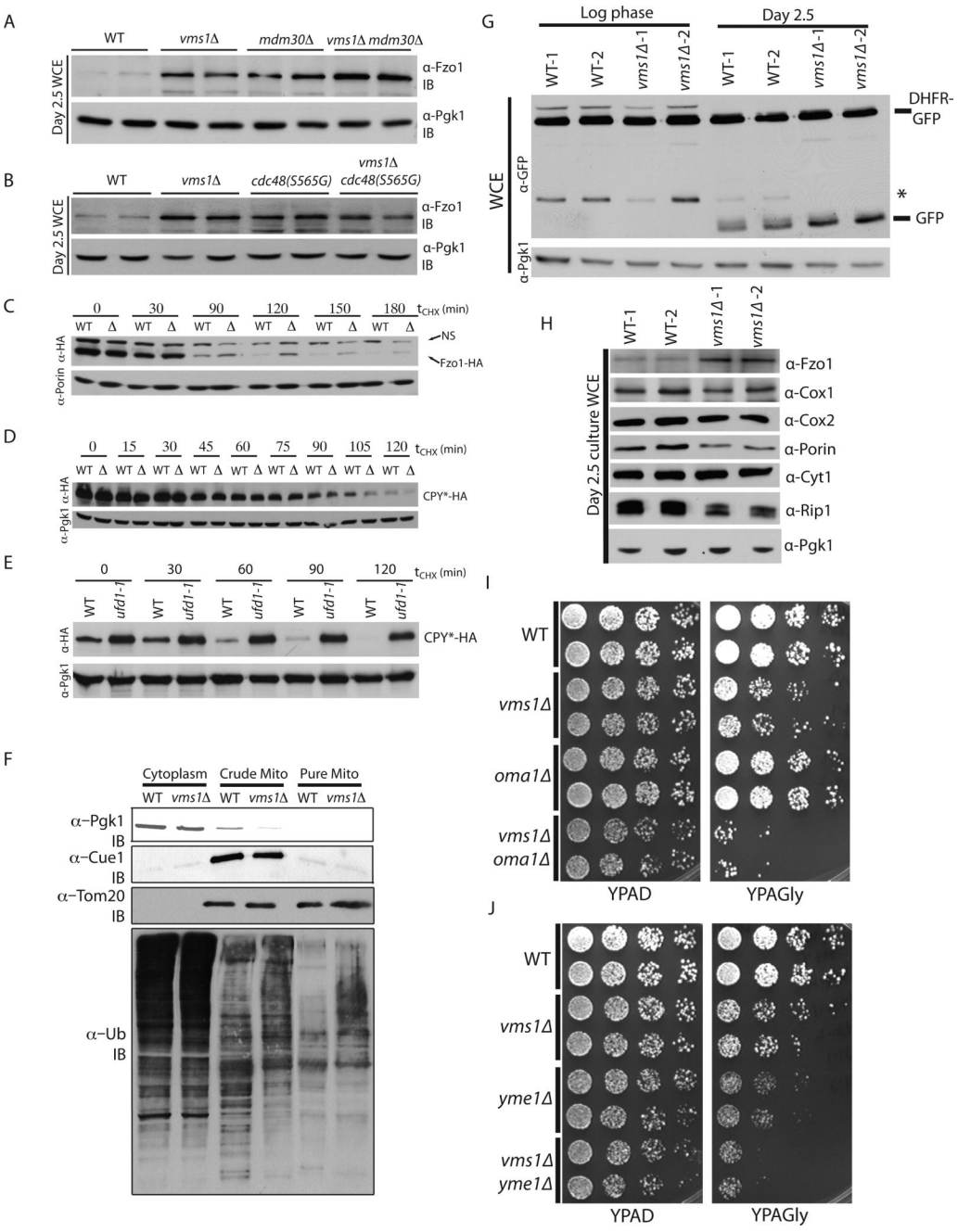

Figure 7. Vms1 is required for normal ubiquitin-dependent mitochondrial protein degradation

(A) WT, *vms1*Δ, *mdm30*Δ, and *vms1*Δ *mdm30*Δ strains were grown in SD complete medium for 2.5 days and whole cell extracts were prepared and subjected to immunoblot using anti-Fzo1 antibody, with anti-Pgk1 being a loading control. (B) WT, *vms1*Δ, *cdc48-S565G*, and *vms1*Δ *cdc48-S565G* strains were treated as in (A). (C) WT and *vms1*Δ strains expressing an HA-tagged allele of Fzo1 were grown to log phase and treated with 0.1 mg/ ml cycloheximide. At the times indicated, samples were harvested and subjected to immunoblotting using anti-HA and anti-porin antibodies. Please note: cycloheximide causes rapid Vms1 translocation to mitochondria. NS indicates a non-specific band that is present in the absence of the plasmid encoding Fzo1-HA. (D) WT and *vms1*Δ strains expressing

CPY*-HA were treated as in (C). (E) WT and *ufd1-1* strains expressing CPY*-HA were treated as in (C). (F) WT and *vms1*Δ strains were grown in YPD medium for 5 days, harvested, and subjected to mitochondria isolation by differential centrifugation. The crude mitochondrial fraction (Crude Mito) was then loaded on a sucrose cushion to separate mitochondria (Pure Mito) from other membranes. Equivalent amounts of proteins were TCA precipitated and immunoblotted using anti-ubiquitin antibody. Anti-Pgk1, Cue1 and Tom20 were used as a marker and loading control for cytoplasm , ER and mitochondria, respectively. (G) WT and *vms1*Δ strains transformed with DHFR-GFP were grown in SD-Ura medium either to log phase or for 2.5 days. Equivalent numbers of cells were harvested, lysed, and subjected to SDS-PAGE followed by immunoblotting using anti-GFP and anti-Pgk1 (loading control) antibodies. The asterisk indicates a DHFR-GFP fragment that is targeted to mitochondria and is degraded upon mitophagy, similar to full-length DHFR-GFP. (H) Two independent cultures of WT and *vms1*Δ strains were grown in SD complete medium for 2.5 days and equivalent numbers of cells were harvested, lysed, and subjected to immunoblot using the indicated antibodies. (I) WT, *vms1*Δ, *oma1*Δ, and *vms1*Δ *oma1*Δ strains were grown in SD complete medium for 1.5 days. 5-fold serial dilution of equivalent numbers of cells were spotted on both YPAD and YPAGlycerol plates and grown at 30°C. (J) WT, *vms1*Δ, *yme1*Δ, and *vms1*Δ *yme1*Δ strains were analyzed as in (I).